Global Change Biology (2004) **10,** 1689–1706, doi: 10.1111/j.1365-2486.2004.00847.x

Spatial and temporal variability in forest–atmosphere CO_2 exchange

D. Y. HOLLINGER*, J. ABER†, B. DAIL‡, E. A. DAVIDSON§, S. M. GOLTZ‡, H. HUGHES§, M. Y. LECLERC¶, J. T. LEE‡, A. D. RICHARDSON†, C. RODRIGUES‡, N.A. SCOTT§, D. ACHUATAVARIER¶ and J. WALSH‡

*USDA Forest Service NE Research Station, 271 Mast Rd., Durham, NH 03824, USA, †Complex Systems Research Center, University of New Hampshire, Durham, NH 03824, USA, ‡Department of Plant, Soil, and Environmental Sciences, University of Maine, Orono, ME 04469, USA, §Woods Hole Research Center, PO Box 296, Woods Hole, MA 02543, USA, ¶Laboratory for Environmental Physics, University of Georgia, Athens, GA 30223, USA

Abstract

Seven years of carbon dioxide flux measurements indicate that a $\sim$ 90-year-old spruce dominated forest in Maine, USA, has been sequestering $174 \pm 46\,g\,C\,m^{-2}\,yr^{-1}$ (mean $\pm$ 1 standard deviation, nocturnal friction velocity (u_*) threshold $> 0.25\,m\,s^{-1}$). An analysis of monthly flux anomalies showed that above-average spring and fall temperatures were significantly correlated with greater monthly C uptake while above-average summer temperatures were correlated with decreased net C uptake. Summer months with significantly drier or wetter soils than normal were also characterized by lower rates of C uptake. Years with above-average C storage were thus typically characterized by warmer than average spring and fall temperatures and adequate summer soil moisture.

Environmental and forest–atmosphere flux data recorded from a second tower surrounded by similar forest, but sufficiently distant that flux source regions ('footprints'), did not overlap significantly showed almost identical temperature and solar radiation conditions, but some differences in energy partitioning could be seen. Half-hourly as well as integrated (annual) C exchange values recorded at the separate towers were very similar, with average annual net C uptake differing between the two towers by $< 6\%$. Interannual variability in net C exchange was found to be much greater than between tower variability. Simultaneous measurements from two towers were used to estimate flux data uncertainty from a single tower. Carbon-flux model parameters derived independently from each flux tower data set were not significantly different, demonstrating that flux towers can provide a robust method for establishing C exchange model parameters.

Keywords: AmeriFlux, carbon exchange, eddy covariance, long-term measurements

Received 26 February 2004; received in revised form and accepted 11 May 2004

Introduction

The eddy covariance technique has played a vital role in improving our understanding of ecosystem physiology and the functioning of the carbon cycle (Running *et al*., 1999; Baldocchi, 2003). However, several uncertainties are presently limiting broader interpretation and use of ecosystem–atmosphere carbon dioxide (CO_2) flux data. For example, studies have demonstrated variation in annual net ecosystem C exchange (NEE) (Goulden *et al*., 1996a; Barford *et al*., 2001; Aubinet *et al*., 2002; Barr *et al*., 2002), but it has been difficult to rigorously (statistically) attribute this C exchange variation to concomitant variation in climatic factors. Part of the problem lies with the complexity of ecosystem response to the environment; annual carbon exchange depends upon the integrals of both photosynthetic uptake and respiratory loss. Differences in the integration period (season length), interannual variation in the factors that affect photosynthesis and respiration (e.g. light, temperature, and water availability), and variation in the biological responses to these environmental factors all contribute to differences

Correspondence: David Y. Hollinger, tel. + 1 603 868 7673, fax + 1 603 868 7604, e-mail: dhollinger@fs.fed.us

in NEE. Without specific attribution, however, it is difficult to reject the null hypothesis that observed interannual variability simply represents 'noise' in either the functioning of the ecosystem, the flux measurement system, or some combination. An alternative approach is to test for correlation in two independent measurements of C flux recorded, for example, at two separate towers. A high degree of statistical significance in that correlation would give us confidence that the observed variations were real, even if we did not completely understand their cause.

Related to this are questions about how well flux values obtained at one location characterize the overall response of the ecosystem under study. For example, how spatially relevant are the single-tower estimates emerging from the C-flux networks? Another way to frame this question is, how robust are model parameter values inferred from flux data? Would an independent data set yield similar C-flux model parameters?

Here, in an effort to address these questions, we compare results from two independent flux systems and explore the larger question of the causes of interannual variability in forest NEE. We investigate interannual variability by correlating climatic and carbon-flux anomalies and also by parameterizing a model using 1 year of flux data, then testing the ability of the model to predict NEE in subsequent years.

Seven years of ecosystem–atmosphere CO_2-flux measurements were made using the eddy covariance technique over spruce-hemlock vegetation at the Howland AmeriFlux site near the southern ecotone of the boreal forest in eastern North America. For 3 years, we obtained concurrent data from a second flux tower located in similar vegetation but $\sim$ 775 m away from our main tower. Previous work shows this to be a suitable site for flux measurements (Hollinger *et al*., 1999).

Methods

Site description

Studies were carried out at the Howland Forest AmeriFlux site located about 35 miles north of Bangor, ME, USA (45°15′N, 68°44′W, 60 m a.s.l.). This site is commercial forestland owned by the International Paper Company Ltd. Forest stands are dominated by red spruce (*Picea rubens* Sarg.) and eastern hemlock (*Tsuga canadensis* (L.) Carr.) with lesser quantities of other conifers (primarily balsam fir, *Abies balsamea* (L.) Mill., white pine, *Pinus strobus* L., and northern white cedar, *Thuja occidentalis* L.) and hardwoods (red maple, *Acer rubrum* L. and paper birch, *Betula papyrifera* Marsh.). Fernandez *et al*. (1993) and Hollinger *et al*. (1999) have previously described the climate, soils, and vegetation at Howland.

For this study, we characterized forest vegetation (tree species and diameter) in 48 plots around each of two research towers. Plots were 7.315 m in radius and followed the design of the USDA Forest Service Forest Inventory and Analysis (FIA) subplots (US Department of Agriculture, Forest Service, 2002). An FIA 'plot' normally consists of three subplots arranged in a triangle (36.6 m between centers) with a fourth subplot in the center of the triangle. Our plots were located on 30° azimuth lines at 50, 100, 200, and 400 m distance from each tower. Total and foliage biomass in these plots were calculated using the allometric equations of Young *et al*. (1980).

The research towers were separated by $\sim$775 m and instrumented with identical eddy covariance systems. The first flux tower ('main' tower, 45.20407°N, 68.74020°W) was established in 1995 and the second ('west' tower, 45.20912°N, 68.74700°W) in 1998.

Flux measurements, calculations, and corrections

Fluxes were measured at a height of 29 m with systems consisting of model SAT-211/3 K 3-axis sonic anemometers (Applied Technologies Inc., Longmont, CO, USA) and model LI-6262 fast response CO_2/H_2O infrared gas analyzers (LiCor Inc., Lincoln, NE, USA), with data recorded at 5 Hz. Precise timebase cards (model NTR2000-P, Kontron, San Diego, CA, USA) kept the flux systems synchronized to within 10 s. The clocks on the data loggers used to record environmental data (model 21X, Campbell Scientific Inc., Logan, UT, USA) were adjusted approximately monthly. The flux measurement systems and calculations are described in more detail in Hollinger *et al*. (1999). CO_2 and H_2O fluxes were corrected for high-frequency losses in the measurement system (damping in the tubing and analyzer) following the procedure of Goulden *et al*. (1996b). This involves online calculation of sensible heat fluxes calculated with sonic anemometer temperature signals that have been digitally filtered to match the frequency response of the CO_2 and H_2O channels. Specifically, half-hourly CO_2 and water vapor fluxes are multiplied by H/H_{fn} where H is the heat flux calculated with the unfiltered sonic temperature and H_{f1} and H_{f2} are heat fluxes calculated with temperature signals filtered to match the high-frequency cutoff of the IRGA channels. This approach has the advantage of not assuming any particular spectral shape but does assume cospectral similarity between the fluxes. To correct for low-frequency losses in heat, water vapor, and CO_2 fluxes resulting from a running mean filter (600 s) and half-hourly block averaging (Sakai *et al*.,

2001), we used the Horst/Massman approach of calculating a transfer function based on stability and theoretical spectra (see also Moore, 1986; e.g. Horst, 1997, 2000; Massman, 2000, 2001). The equations in Massman (2001), Table 1 were used but with p, the term accounting for high-frequency corrections, set to zero. Our correction philosophy is thus a hybrid, using a spectral model and transfer function to correct for missing low-frequency contributions and a ratio of filtered to unfiltered heat fluxes to account for missing high-frequency fluctuations. Average high- and low-frequency CO_2-flux corrections in the daytime were 5.6% and 6.8%, respectively, and at night, 10.1% and 7.9%. A spreadsheet with our implementation of the Horst/Massman spectral corrections is available from the first author.

Half-hourly flux values were excluded from further analysis if the wind speed was below $0.5\,m\,s^{-1}$, sensor variance was excessively high or extremely low (Hollinger *et al*., 1995), rain or snow was falling, half-hour sample periods were incomplete or in case of instrument malfunction. The sign convention used here is that carbon flux into the ecosystem is defined as negative.

At night, a stable atmosphere often limits the applicability of the eddy covariance approach (Hollinger *et al*., 1994; Black *et al*., 1996; Goulden *et al*., 1996a; Lee, 1998). Hollinger *et al*. (1994) identified stable layer formation and breakdown as a cause of intermittent nocturnal CO_2 flux, and showed that CO_2 efflux from a forest increased with increasingly negative sensible heat flux (downward transport of warm, unstable air). Goulden *et al*. (1996a) introduced the idea of a friction velocity threshold, $(u_* = \sqrt{\overline{w'u'}})$ where nocturnal CO_2-flux data were only accepted as valid when they exceeded a predetermined value (in the case of Goulden *et al*., 1996 of $0.2\,m\,s^{-1}$). This approach is now generally accepted (Hollinger *et al*., 1999; Aubinet *et al*., 2002; Barr *et al*., 2002; Carrara *et al*., 2003). There is potential concern about how somewhat arbitrary nocturnal u_* thresholds affect integrated estimates of CO_2 exchange, and we address this issue in the Appendix.

To obtain annual estimates of C exchange, values missing from the half-hourly record of annual NEE were modeled by combining estimates of canopy photosynthesis and nocturnal respiration. Daytime CO_2 exchange rates were obtained from Michaelis–Menten models of photosynthetically active photon flux density (PPFD) with coefficients fitted on a monthly basis. Missing nocturnal CO_2 exchange values were obtained from second-order Fourier regressions between Julian day (JD) and nocturnal respiration. Fourier regressions have several advantages over temperature-driven exponential relationships including a lack of bias, no need for external driving data, and similar or higher R^2 values.

Footprint calculations

The flux footprint is the contribution per unit emission from each element of a surface area source to the vertical scalar flux measured at a certain height above the surface (Horst & Weil, 1992). In this analysis, the footprint estimations are carried out using the simple analytical footprint model proposed by Horst & Weil (1994). Despite its simplicity, this model uses height-dependent wind and eddy-diffusivity profiles and is evaluated against direct observations above canopies of various roughness (Finn *et al*., 1996; Leclerc *et al*., 2003a, b). Horst & Weil (1994) showed the crosswind-integrated footprint; $\bar{f}^y(x, z_m)$ as a function of $\bar{z}/z_m$, where $\bar{z}$ is the mean plume height and z_m is the measurement height:

$$\bar{f}^y(x, z_m) = \left(\frac{z_m}{\bar{z}}\right)^2 \frac{\bar{u}(z_m)}{U(\bar{z})} A e^{-(z_m/b\bar{z})^s}. \quad (1)$$

The mean horizontal wind speed $(\bar{u})$ is obtained from the logarithmic profile and the mean plume speed (U) is calculated as the wind speed at a fraction (c) of the mean plume height. The constant s is the shape factor and is taken as 1 in unstable, 1.5 in near neutral and 2 in stable conditions and A and b are functions of s. The dependence of the footprint on stability, surface roughness and measurement height is contained in the dependence of these quantities on $\bar{z}/z_m$. The inputs for the model are measurement height, canopy height (h), roughness length $(0.1h)$, displacement length $(0.75h)$, Obukhov length (L) and friction velocity (u_*).

Statistical analyses

We used a commercial data analysis package (COPLOT, CoHort Software, 2002) for calculation of means, Pearson's product moment correlation coefficients, analysis of variance, and linear and nonlinear regression analyses using least-squares techniques. Reduced major axis (RMA) regressions were calculated with the PAST program (Hammer *et al*., 2001). In the text, we refer to coefficients of determination from regression analysis as 'R^2' values and Pearson's product moment correlation coefficients as 'r' values.

To examine the two-tower correlation of environmental or flux data as a function of frequency (coherence spectra, von Storch & Zwiers, 1999), we used a computer program developed by Carter & Ferrie (1979). Time periods of 512 contiguous half-hourly (PPFD) or 15 min (T_{air}, CO_2 concentration, fluxes) data without any missing values were selected for these

analyses. To calculate maximum likelihood (ML) parameter estimates, we used the Monte Carlo method (Metropolis *et al*., 1953) to minimize the sum of squares of the weighted differences between measured and modeled values (Press, 1993).

Results

Forest characteristics

Forest plots around the towers were dominated by red spruce and eastern hemlock, which together accounted for about 69% of the live basal area. Faster growing species including red maple, birch, and white pine, together accounted for 17% of the live basal area and the slower growing northern white cedar for most of the rest. Mean live basal area in plots around the west tower at $56.7 \pm 16.5\,m^2\,ha^{-1}$ (mean and standard deviation) was somewhat higher than around the main tower ($47.6 \pm 16.6\,m^2\,ha^{-1}$, $t = 2.07$, $P < 0.05$). Closer inspection of the data shows that basal area of plots near both towers was similar, but that plots 400 m from the main tower had values lower than similarly distant plots around the west tower. This difference was mostly because of several plots located east of the main tower that fell in stands harvested within the past 20 years. Mean basal area of plots close to both towers was not significantly different ($54.4 \pm 14.0\,m^2\,ha^{-1}$ main tower, $59.1 \pm 13.2\,m^2\,ha^{-1}$ west tower, $t = 1.18$, $P = 0.24$).

Total and foliage biomass on plots around the main tower ($119.7 \pm 47.1\,t\,C\,ha^{-1}$ total, $9.7 \pm 3.8\,t\,C\,ha^{-1}$ foliage biomass) were significantly less (*t*-tests, $P < 0.05$) than on plots around the west tower ($150.8 \pm 58.5\,t\,C\,ha^{-1}$ total, $11.5 \pm 3.2\,t\,C\,ha^{-1}$ foliage biomass). Plots within 50 m of the towers were similar, but plots 100–400 m from the west tower contained, in general, fewer, larger trees than those around the main tower, accounting for the similarity in basal area but difference in standing biomass.

Nocturnal CO_2 fluxes

In a previous study (Hollinger *et al*., 1999), we omitted Howland nocturnal CO_2-flux values from further analysis when the friction velocity, u_*, was below $0.15\,m\,s^{-1}$. With six additional years of data, we revisited this decision (see Appendix) and now conclude that a higher u_* threshold of $0.25\,m\,s^{-1}$ is justified, but because of uncertainties in setting the threshold, we bracket our estimates of NEE with similar calculations using u_* thresholds of 0.20 and $0.30\,m\,s^{-1}$. The result of this decision is to decrease the NEE value previously reported at Howland (Hollinger *et al*., 1999) by $\sim 25\%$.

Spatial variability in environmental variables and fluxes. We did not expect to see systematic differences in average environmental measurements recorded on towers at the same elevation and separated by only 775 m (Table 1). Comparing data recorded in 2000, half-hourly air temperature and incoming PPFD values from the towers are nearly identical (slopes close to 1 and very high R^2 values, RMA regressions). The 1.8 °C offset in air temperatures between the two towers represents an offset between the precision sensor at the main tower and the sonic anemometer temperature recorded at the west tower. Similarly, the deviation of slope in the PPFD relationship from 1.0 is most likely indicative of calibration variation between the sensors. The systematic difference in net radiation recorded at the two towers as indicated by the 1.113 slope (Table 1) is greater than any expected calibration error. However, the footprint of these instruments is small (Schmid, 1994) and we suspect it is unlikely that these differences are indicative of differences in the larger footprint region associated with latent and sensible heat flux around the towers.

On a half-hourly basis, wind speed and precipitation are more variable across ~ 800 m than radiation or temperature as indicated by the lower R^2 values. Although the slope in the precipitation relationship is close to 1.0, we found that in summer, rainfall amounts from individual convective storms may differ by over 50% between the towers.

Half-hourly values of u_*, H, and LE measured simultaneously from the two towers are also similar, but with lower R^2 values than temperature or radiation data (Table 1). The coefficients of determination for u_* readings made in the day or at night were similar (0.85 vs. 0.83). For heat flux, the deviation in the slope of the relationship between the two towers (> 1.0) is matched by a reciprocal decrease in latent heat flux (slope < 1.0) suggesting that energy balance is maintained by a different partitioning between H and LE at the two towers. Comparing heat flux values recorded at the two towers during winter months when transpiration is absent because of frozen soil supports this conclusion (Table 1), as the slope of the relationship is not significantly different from unity ($P = 0.24$). If we assume that transpiration per unit mass foliage is constant, this difference in energy partitioning (higher LE recorded by the west tower) can be explained by the greater canopy biomass around the west tower than the main tower. Overall energy balance at the two towers was similar, at the main tower $H + LE = 0.93R_n - 2.1$, while at the west tower $H + LE = 0.89R_n - 7.2$ (RMA regressions).

CO_2 fluxes recorded at both towers are similar on a half-hourly or daily integral basis (Fig. 1). For

Table 1 Relationship between environmental variables or fluxes measured over the same half-hour time periods at the main and west towers at Howland in 2000

Variable	Slope (SE)	Intercept (SE)	R^2	n
T_{air} (°C)	0.998 (0.001)	1.797 (0.009)	0.998	10 064
PPFD (μmol $m^{-2} s^{-1}$)	1.043 (0.002)	−0.88 (1.20)	0.993	6833
R_n (W m^{-2})	1.113 (0.001)	1.76 (0.31)	0.992	10 069
$\bar{u}$ (m s^{-1})	0.871 (0.004)	0.071 (0.024)	0.845	8944
Precipitation (mm)	0.974 (0.005)	−0.001 (0.001)	0.876	10 717
u_* (m s^{-1})	0.952 (0.004)	−0.011 (0.004)	0.844	8944
H (W m^{-2})	1.107 (0.003)	0.67 (0.36)	0.901	11 724
H (days 1–60 only)	1.011 (0.009)	−0.37 (0.66)	0.834	2073
LE (W m^{-2})	0.849 (0.004)	2.31 (0.30)	0.752	12 242
FCO_2 (μmol $m^{-2} s^{-1}$)	0.894 (0.004)	−0.116 (0.030)	0.830	7309
FCO_2 (day)	0.894 (0.006)	−0.155 (0.056)	0.785	4901
FCO_2 (night)	0.804 (0.010)	0.158 (0.044)	0.623	2408

Main = West × slope + intercept, RMA method. For CO_2 flux, $u_* > 0.25$ at both towers.
RMA, reduced major axis; PPFD, photosynthetically active photon flux density; SE, standard error.

half-hourly CO_2-flux data (Table 1), the difference of the slope from 1.0 is consistent with that of the water vapor flux, and can possibly be interpreted as resulting from the greater canopy mass around the west tower than the main tower. The relationship suggests that forest around the west tower has a greater rate of daytime uptake, as well as larger nocturnal losses, than similar forest around the main tower. Since these factors will have opposite effects on NEE, the consequence of the differences between towers on integrated NEE is not clear.

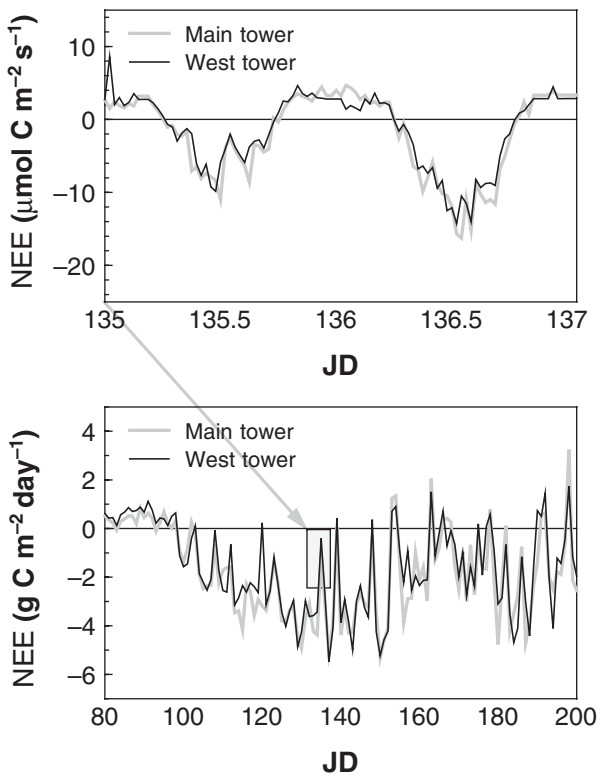

Fig. 1 Net ecosystem C exchange (NEE) fluxes recorded at two towers separated by ~ 775 m are correlated over short term as well as long term.

With $u_* > 0.25$, over 80% of the variance in half-hourly fluxes in one tower could be accounted for in data from the other tower. This is significantly more of the variance than can typically be accounted for by simple models based on light and temperature (Goulden *et al*., 1997; Hollinger *et al*., 1998). At night, the strength of the correlation of CO_2 fluxes between the towers depended upon atmospheric mixing. With good mixing (nocturnal $u_* > 0.25$ at both towers), the correlation coefficient for CO_2 exchange (r) was 0.79 ($n = 2409$). However, when atmospheric mixing was poor (e.g. $u_* < 0.25$ at both towers) or for the less frequent patchy case ($u_* > 0.25$ at one tower but < 0.25 at the other), the correlation of CO_2 fluxes was considerably lower (poor mixing, $r = 0.64$, $n = 2359$; patchy mixing, $r = 0.45$, $n = 558$).

The 775 m distance between the towers was chosen to ensure that the towers are generally integrating fluxes from different patches of forest (e.g. the towers are recording data from distinct footprints). When the wind is blowing along the axis between the towers, however, overlap may occur. Using the Horst model described earlier, we analyzed cases when the wind direction ($\bar{\theta}$) was along the axis between the towers (between 130–140° or 310–320°). Over the 1996–2001 period, the wind blew along this range of wind directions (e.g. along the axis between the towers) only 9.4% of the time. Even when the wind did blow

along the line of the towers, the footprint model suggests that overlap was minimal. Using wind and stability data from July 2001 as a representative time period, the model indicates daytime along-axis overlap of <1.5% and nocturnal footprint overlap of <15%. We are thus obtaining similar fluxes from both towers because different patches of forest are responding similarly, not because the two towers are measuring the same patch of forest.

For air temperature (Fig. 2a), data from the two towers were highly correlated (coherence >0.95) for all frequencies $<10^{-4}$ Hz (about 3 h). However, high-frequency fluctuations were less tightly correlated between the towers than lower frequency fluctuations. For PPFD (Fig. 2a), the between-tower coherence is essentially unity for frequencies $< \sim 6\times10^{-5}$ Hz (about 4.5 h), drops to 0.7–0.8 for frequencies between $\sim 6\times10^{-5}$ and $\sim 2\times10^{-4}$ Hz (4.5–1.5 h) and decreases further at higher frequencies. The coherence spectra of air temperature and PPFD can be understood by considering the spatial scale of the different factors affecting these power spectra. The diurnal motion of the sun and passage of frontal systems are coherent across hundreds of kilometers and both strongly influence air temperature and PPFD at frequencies lower than $\sim 10^{-5}$ s (1 to many days). The afternoon development of fair weather clouds or clearing of morning fog occurs at a somewhat higher frequency ($\sim 10^{-5}$ to $\sim 10^{-4}$ s; less than a day but greater than a few hours). The spatial scale of these changes is also large (many 10's of km). Variation of air temperature and PPFD at the highest frequencies is associated with shadows produced by wind-driven cumulus clouds (O'Brien, 1987). Because the size of these clouds is similar in magnitude to the distance between the towers, coherency between towers at higher frequencies is reduced. Coherence at higher frequencies is also more sensitive to the timing of the measurements. If one datalogger ends a half-hour time period 2 min ahead of another, they will share only 87% of the data record.

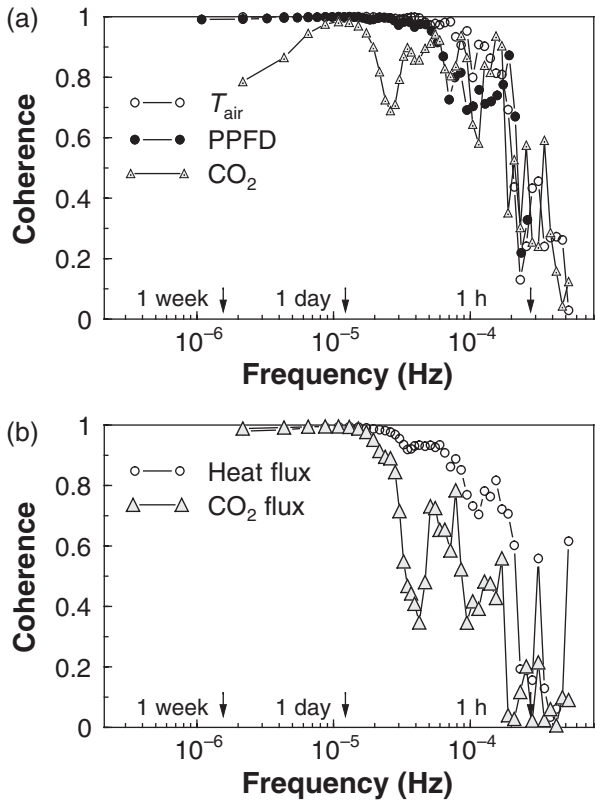

Fig. 2 (a) Coherence spectra for environmental variables recorded by systems on two towers separated by $\sim$ 775 m show that fluctuations down to several hours are highly correlated. (b) Similar analysis for heat and carbon dioxide (CO_2) fluxes indicate that even relatively high-frequency flux variations are correlated.

Variations in CO_2 concentration are also coherent across the 775 m separating the towers at a range of frequencies. Coherence is near unity for diurnal ($\sim 10^{-5}$ Hz) fluctuations and remains high up to $\sim 4\times10^{-4}$ Hz (3 h scale). The relatively high between-tower coherence in CO_2 concentration over the shorter time period is probably driven by the coherent changes in PPFD across the region, the dynamics of the boundary layer, and the efficient turbulent mixing of the atmosphere. We hypothesize that regionwide changes in PPFD drive changes in NEE that affect regionwide CO_2 concentration. This interpretation is supported by the dip in CO_2 coherence at $\sim 2.3\times10^{-5}$ Hz (12 h), which results from nocturnal values being less correlated than daytime values (Fig. 2a).

The coherence spectrum of heat flux measurements made simultaneously at both towers (Fig. 2b) is very similar to that of PPFD measurements, illustrating the direct link between incoming radiation and heat flux. For CO_2 flux, the coherence spectrum indicates high values for frequencies $< \sim 1.16\times10^{-5}$ Hz (>1 day), a dip between $\sim 2.3\times10^{-5}$ and 5×10^{-5} Hz (6–12 h), moderate values between 5×10^{-5} and 1.8×10^{-4} Hz (1.5–6 h) and a loss of coherence above $\sim 1.8\times10^{-4}$ Hz (<1.5 h). The CO_2-flux coherence spectrum (Fig. 2b) is similar to the PPFD spectrum combined with the reduction around 2.5×10^{-5} Hz seen in the CO_2 concentration spectrum. We interpret this as indicating that most of the time CO_2 flux is regulated by relatively large-scale variations in PPFD but that at night small-scale differences in transport become important.

The CO_2-flux coherence seen in the short-term (7 days) analysis is maintained over the course of a season and several years (Figs 1 and 3). Remarkably, on an

annual basis, NEE observed at the two towers differed on average by less than 6% (Fig. 3). An analysis of variance (Table 2) indicates that the temporal (year-to-year) variability is much greater than the spatial (between-tower) variability.

Recovering model parameters from flux data

To explore how well model parameters could be recovered from flux data, we fit half-hourly daytime (PPFD $> 5\,\mu mol\,m^{-2}\,s^{-1}$) NEE data to a simple model of PPFD on a monthly basis using light data from the main tower and independent flux data from each tower. A nonlinear least-squares approach (CoHort Software, 2002) was used with data from March to November in 1999–2001 and a simple three-parameter model consisting of the Michaelis–Menten relationship describing saturating enzyme kinetics with a constant rate of respiration:

$$\mathrm{NEE} = P_{\max} I/(I + K_m) + R_d, \qquad (2)$$

where I is the incident PPFD, P_{max} is the maximum rate of CO_2 uptake, K_m is the PPFD at which NEE $= 0.5P_{max}$ and R_d is the nocturnal (dark) respiration. We use this as a simple example to compare results from the independent (two tower) data streams. We evaluate a slightly more complicated model later.

For these data, the independent recovery of surface flux model parameters from each tower's data record was robust. All of the model parameters (P_{max}, K_m, R_d) derived on a monthly basis from one tower were highly correlated with those derived from the other tower (for P_{max}, $r = 0.98$; K_m, $r = 0.71$; R_d, $r = 0.98$; in each case $P < 0.001$). The mean differences in model parameters calculated as (Main−West)/Main were remarkably small. For P_{max}, K_m, and R_d the mean (± 95% confidence interval) differences in monthly model parameters derived from the two towers were 9.4 ± 4.1%, 13.0 ± 8.7%, and 4.1 ± 8.7%, respectively. The differences between P_{max} and K_m coefficients derived from the main and west towers were small but significantly different from zero whereas the R_d values were not significantly different. Because P_{max} and K_m are not completely independent (see next section), we compared gross ecosystem exchange (here GEE $= P_{max} I/(I + K_m)$) at a PPFD of $1000\,\mu mol\,m^{-2}\,s^{-1}$ as well as R_d derived from the two towers (Fig. 4). When evaluated at $1000\,\mu mol\,m^{-2}\,s^{-1}$, models derived from each tower on a monthly basis yielded GEE values that were not significantly different (difference of 3.6 ± 5.6%, mean ± 95% confidence interval).

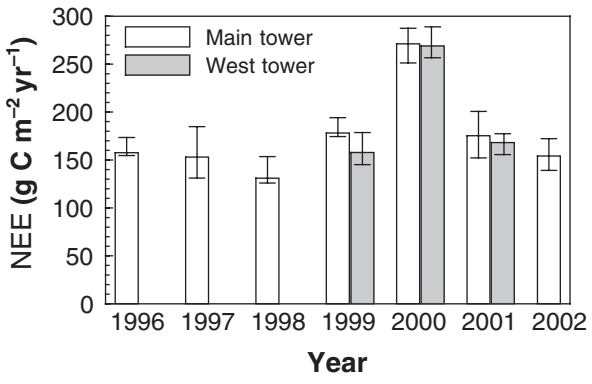

Fig. 3 Interannual variability of net ecosystem C exchange (NEE) at Howland is greater than the spatial variability observed by two towers in similar forest separated by ~ 775 m.

Table 2 Analysis of variance of interannual and between-tower net ecosystem C exchange (NEE)

Source	Degrees of freedom	Sum of squares	*F*-value	*P*
Year	2	13 571	89.2	0.011
Tower	1	148	1.9	0.30
Error	2	152		

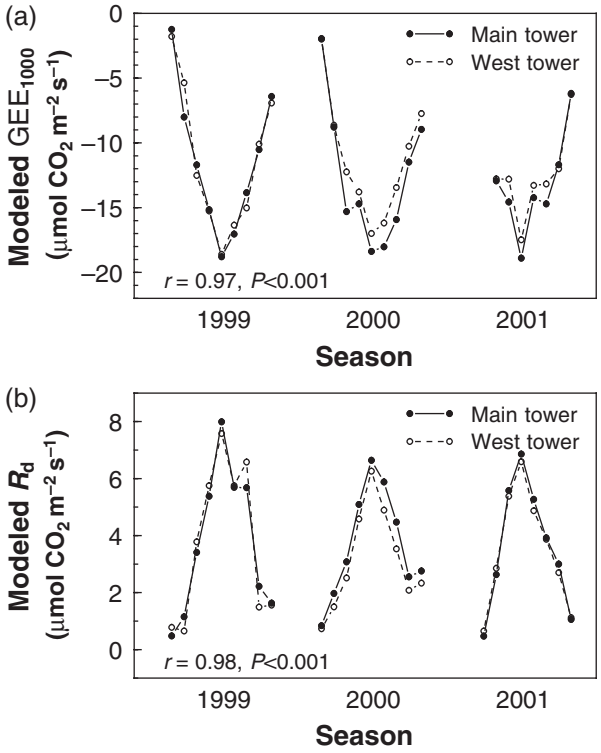

Fig. 4 Modeled GEE and nocturnal respiration obtained from simple models parameterized by independent data obtained from separate flux towers in similar forest.

These small relative differences in monthly parameter values obtained from the separate tower data sets suggest that the much larger seasonal and interannual variations seen in model parameters recovered from flux data (Fig. 4) are indicative of real ecological responses and differences. Using a three-way ANOVA to partition the variance in the model parameters between months, towers, and years, the general patterns are similar for GEE (evaluated at 1000 μmol $m^{-2} s^{-1}$ PPFD) and R_d. Most of the variation in this analysis is associated with seasonal changes, accounting for 91% of the variance in both of these parameters. The 'year × month' term, meaning differences between the same monthly values in different years (e.g. interannual variability in seasonal changes) accounts for about one-half (GEE) and two-thirds (R_d) of the remaining variance. For GEE, differences between 'towers' and 'years' account for about 14% and 6%, respectively, of the remaining variance while for R_d, the values are about 4% and 16%, respectively. For both GEE and R_d, the 'tower × year' term is also significant and can be seen in Fig. 4 as the offset between the towers that occurs in 2000 but not 1999.

Using data from two towers to estimate uncertainty in flux data

ML methods can be used to provide unbiased estimates of model parameters from experimental data (Bevington, 1969). In the case where sample measurement error is independent, normally distributed, and with a constant (identical) standard deviation for all points, normal least squares provides the ML estimate of the fitted parameters. Generally, flux researchers have implicitly made these assumptions and obtained model parameters with linear or nonlinear least-squares techniques (for a notable exception, see van Wijk & Bouten, 2002). Aside from convenience, the main reason for making these assumptions is lack of information about measurement error in flux data. Published data relating to flux measurement error (error magnitude, variation with environmental conditions, and statistical distribution) are generally not available. With the two towers at Howland, however, we have independent and simultaneous measures of CO_2 flux from which we can derive uncertainty estimates for fluxes from a single tower. We have shown already that the mean difference between simultaneous flux values from the two towers is very close to zero, assuming that the error from both towers contributes equally to the error in the difference, the uncertainty from one tower (expressed as a standard deviation) is simply

$$\sigma = \frac{\sigma_{\text{difference}}}{\sqrt{2}}, \qquad (3)$$

where $\sigma_{\text{difference}}$ is the standard deviation of the difference between the towers over some block of time or conditions (PPFD, wind, etc.). Using this approach, the uncertainty in one-tower half-hourly CO_2-flux measurements, expressed as a standard deviation, increases from an average of 0.7 μmol $m^{-2} s^{-1}$ in winter (January–March) to 2.86 μmol $m^{-2} s^{-1}$ in summer (July–September).

Contrary to least-squares assumptions, the uncertainty is not constant, but varies with the season. Further analysis (Fig. 5) shows that uncertainty is an increasing function of the absolute value of the flux and a decreasing function of wind speed. The finding that uncertainty declines with increasing wind speed is significant but not surprising as it suggests that uncertainty in flux data is directly related to the turbulent regime.

Our findings can be used with ML methods (Press, 1993) to improve parameter estimates derived from flux data. In Fig. 6a, for example, we use ML methods with

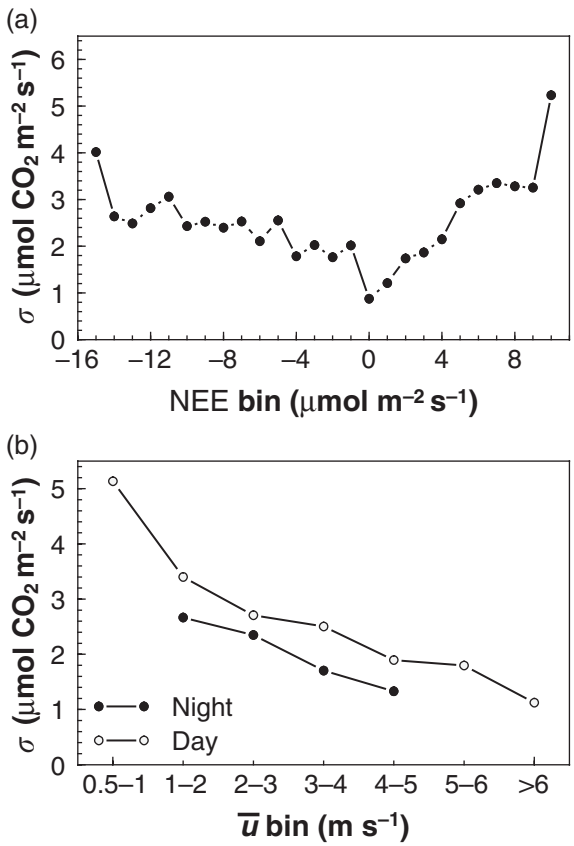

Fig. 5 Uncertainty expressed as a standard deviation of flux measurement error derived from the difference in measurements in two nearby towers. (a) Standard deviation (σ) of data binned according to half-hourly net ecosystem C exchange (NEE) for all of 2000 ($n = 11\,365$). (b) Standard deviation (σ) of data binned according to wind speed for 2000 ($n = 11\,365$).

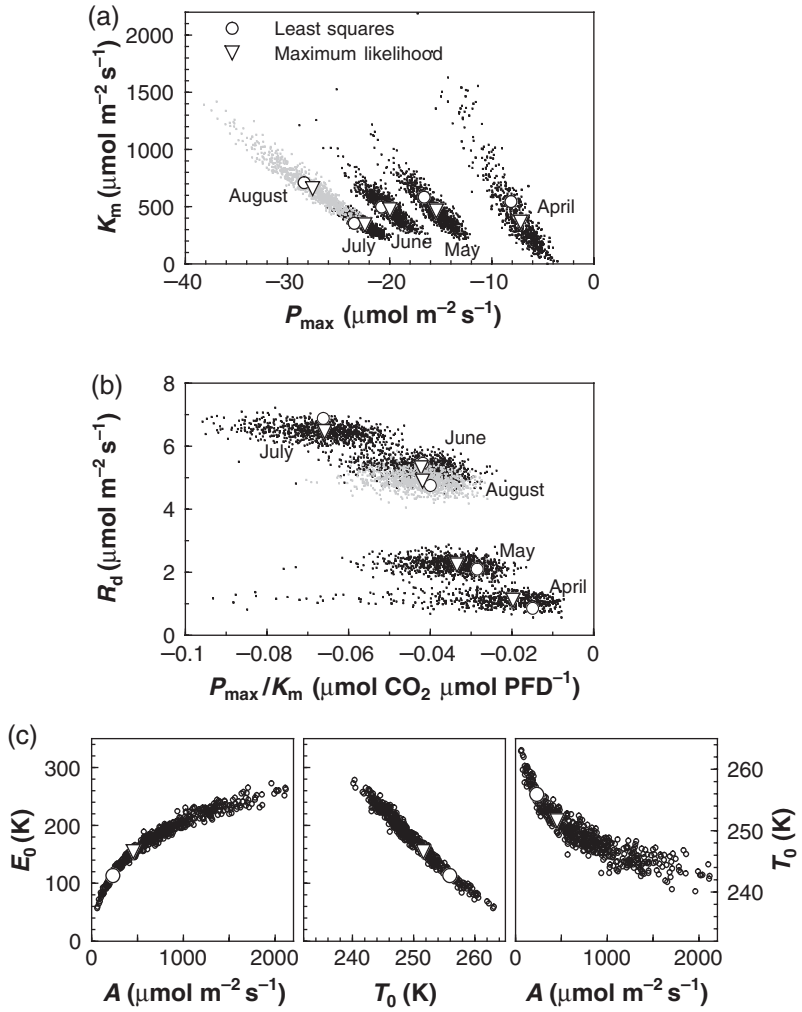

Fig. 6 Maximum likelihood (ML) estimates of parameter values for simple models of photosynthesis ($P = P_{max}I/(I + K_m) + R_d$) and respiration ($R = Ae^{-E_0/(T-T_0)}$). The open circles represent the best fit obtained using a constant uncertainty (equivalent to that obtained via least squares) and the open triangles represent the ML estimate based on uncertainty decreasing with wind speed according to Fig. 5b. The small dots populate the 90% confidence space and were obtained by Monte Carlo simulations. (a) Simultaneous variation in P_{max} and K_m parameters calculated from monthly daytime flux data in 1996. The slopes in the monthly relationships indicate that P_{max} and K_m are strongly correlated (e.g. $r = 0.85$ for June). (b) P_{max}/K_m (ε) vs. R_d for monthly daytime flux data in 1996. August values are shown in gray to help distinguish overlapping data. (c) Simultaneous parameter values for Monte Carlo simulations of the Lloyd & Taylor (1994) respiration model based on 1996 nocturnal flux data. As before, the least-squares solution is indicated by an open circle and ML solution (based on uncertainty decreasing with wind speed) indicated by an open triangle.

constant uncertainty (σ fixed) and with uncertainty that changes with wind speed to obtain two sets of P_{max} and K_m parameter estimates of three-parameter photosynthesis models (Eqn (2)) of daytime NEE data over 5 different months in 1996. Obtaining an estimate of measurement uncertainty allows us to also apply Monte Carlo methods to obtain estimates of parameter uncertainty. In Fig. 6, we use uncertainty that varies with wind speed in a Monte Carlo analysis to generate 1000 other realizations of the 'measurement' data each month that yield a range of model parameter values. The analysis shows that model parameter P_{max} is highly correlated with parameter K_m (r ranging from -0.85 in July to -0.95 in August), which means that we cannot specify independent uncertainties for these parameters (Fig. 6a). Because P_{max} and K_m are tightly correlated, we follow van Wijk & Bouten (2002) and consider the single variable P_{max}/K_m ($= \varepsilon$, the light-use efficiency) (Fig. 6b). The correlation between this parameter and R_d is low (ranging from -0.12 in April to -0.36 in July). This analysis shows that our monthly parameter estimates for April–July are all significantly different

(<5% overlap of the monthly parameter 'clouds') but that August parameter values are not significantly different from those in June. Furthermore, our Monte Carlo simulations show that the 'optimum' parameter values calculated with least-squares assumptions lie well within the 90-percentile cloud of points calculated for the ML estimates and are thus acceptable. For a commonly used respiration model driven by soil temperature (see Eqn (4)), we find that least-squares estimates of parameter values using 1996 nocturnal data when $u_* > 0.25\,\mathrm{m\,s^{-1}}$ are also satisfactory when compared to ML estimates (Fig. 6c). For this model, we again found that there were a number of parameter sets that acceptably fit the observed data.

Estimating model parameters from flux data to predict NEE

Parameter values for ecosystem carbon exchange models have typically come from a variety of short-term laboratory and field experiments and might historically have been characterized as 'data poor'. This is in direct contrast to the quantity of data available from flux sites. Here we establish parameter values for a simple model of NEE based on our first year's (1996) data and use it with environmental data from subsequent years to predict NEE in 1997–2002. Deviations between model results and recorded data provide insight into other significant (nonmodeled) variables and begin to answer questions about how well we can actually predict ecosystem responses to interannual climate variability. We chose a minimally complex six-parameter model to fit to 1996 data. First, we fit a three-parameter model based on soil temperature at 5 cm to nocturnal flux data (under well-mixed nocturnal conditions when $u_* > 0.25\,\mathrm{m\,s^{-1}}$) to estimate ecosystem respiration, R_{eco}. We then used this model in the daytime to estimate GEE ($=\mathrm{NEE}-R_{eco}$) and estimated GEE as another three-parameter model, in this case the product of a rectangular hyperbola (Eqn (2) without the R_d term) in PPFD and a normalized parabolic temperature response. This model was fit with nonlinear least-squares techniques as described previously.

For ecosystem respiration, we used the three-parameter exponential relationship of Lloyd & Taylor (1994) that generally provides a good fit to soil respiration data:

$$R = A\mathrm{e}^{-E_0/(T-T_0)}, \quad (4)$$

where R is respiration, A is a scaling factor (maximum rate), E_0 is a temperature (K) that affects the shape of the curve, and T_0 is a temperature between 0 K and T. An advantage of this relation is that it is sigmoidal and thus better behaved than a simple exponential beyond the domain of parameterization.

Our complete model is driven by the incident PPFD (I), air and soil temperatures (T_{air} and T_{soil}) and contains parameters for the maximum rate of photosynthesis (P_{max}), photosynthetic half-saturation constant (K_m), normalized parabolic temperature response with an intercept of 0 (a), and respiration parameters (A, E_a, and T_0) as described previously:

$$\mathrm{NEE} = \frac{P_{max} I}{I + K_m}\left(\frac{-a^2 T_{air}}{4} + a T_{air}^2\right) + A\mathrm{e}^{-E_a/(T_{soil}-T_0)}. \quad (5)$$

To account for winter inhibition on photosynthesis, if T_{air} or T_{soil} $<0\,^{\circ}\mathrm{C}$ then only respiration is calculated. The least-squares fit of the respiration model (Eqn (4)) to 1996 nocturnal half-hourly data (Fig. 7) was good ($R^2 = 0.55$, root mean square error (RMSE) = $1.25\,\mu\mathrm{mol\,m^{-2}\,s^{-1}}$) with integrated (annual sum) modeled respiration about $12\,\mathrm{g\,C\,m^{-2}}$ (2.7%) less than the measured 1996 value. Model coefficients were $A = 231.0\,\mu\mathrm{mol\,m^{-2}\,s^{-1}}$, $E_0 = 113.4\,\mathrm{K}$, and $T_0 = 255.9\,\mathrm{K}$ (Fig. 6c). During the daytime, the model fit (Eqn (5)) was also good ($R^2 = 0.66$, RMSE = $3.30\,\mu\mathrm{mol\,m^{-2}\,s^{-1}}$) with the modeled annual daytime sum of carbon uptake 5.5% below measured values. The coefficient values were physiologically reasonable with $P_{max} = -22.4\,\mu\mathrm{mol\,m^{-2}\,s^{-1}}$, $K_m = 324\,\mu\mathrm{mol\,photons\,m^{-2}\,s^{-1}}$, and a photosynthetic temperature optima of 25.8 °C. The modeled annual NEE for 1996 of $-136.2\,\mathrm{g\,C\,m^{-2}}$ is ~14% below the observed value of $-157.6\,\mathrm{g\,C\,m^{-2}}$.

However, an examination of Fig. 7 shows that in 1996 net uptake began sooner than predicted, was over-predicted by the model in early spring (JD 110–140), and somewhat under-predicted in summer (JD 180–270). Analysis of the residuals in the fit to 1996 data confirmed that the largest amount of the remaining

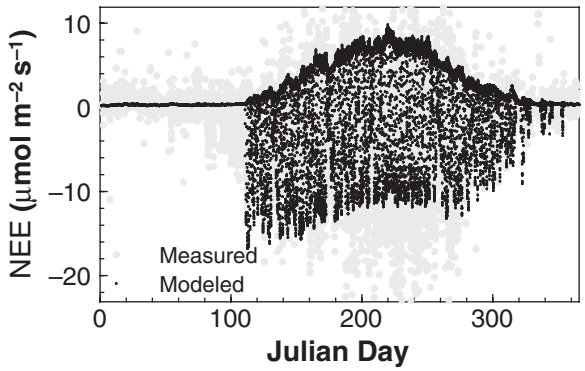

Fig. 7 Comparison of measured (gray symbols) and modeled (dark symbols) half-hourly net ecosystem C exchange (NEE) data in 1996. The modeled data do not adequately capture the seasonal variation in maximum daily uptake.

variance ($\sim 10\%$ of nocturnal and 15% of daytime residuals) was associated with the JD, suggesting that seasonal changes in the ecosystem state influenced parameter values. For example, a model with a P_{max} that increased and then decreased over the season (see Fig. 6a) would have provided a better fit to the data than the current model. Other factors excluded from the model such as daytime saturation deficit or wind direction were less important, being associated with $<5\%$ of the residual variance.

Using the parameter values established from the 1996 flux data and half-hourly meteorological data from subsequent years, we estimate mean annual NEE over the 1997–2002 period of $-175.5 \pm 34.9\,g\,C\,m^{-2}\,yr^{-1}$ (mean and standard deviation based on a u_* threshold of $0.25\,m\,s^{-1}$), which compares well with the 'measured' mean of $-174 \pm 46\,g\,C\,m^{-2}\,yr^{-1}$ (Table 3). (We note here that 'measured' NEE and respiration consist of a combination of measured and modeled (filled) data and that GEE is derived from subtracting modeled daytime respiration from NEE.) Closer inspection (Fig. 8) reveals a more complicated picture. Neither modeled annual respiration, GEE, nor NEE are significantly correlated with their 'measured' counterparts over the 1996–2002 period (respiration, $r = 0.45$, $P = 0.32$; GEE, $r = 0.46$, $P = 0.30$; NEE, $r = 0.06$, $P = 0.91$); our model has failed to adequately predict C exchange at this time scale. Despite the poor fit between annual model estimates based on 1996 parameters and 'measured' values, some patterns are visible in the data. For respiration, all values are under-predicted with the error more severe in years after 1997. The large jump in measured respiration in 1998 was ecosystem behavior not captured by the model. Interestingly, a record ice-storm struck the site in January of 1998 felling many smaller standing dead trees and breaking branches. This input of coarse and fine woody debris early in 1998 to the soil pool would be consistent with the observed increase in respiration. For GEE, the model also under-predicts although this is at least in part a consequence of the under-prediction of respiration. Measured and modeled GEE values are correlated with the exception of 2000, when measured C uptake was substantially above the modeled value. The cause of such a spike above predicted values is not readily apparent.

Table 3 Components of ecosystem carbon exchange at the Howland site

Year	NEE	R_{eco} (night)	R_{eco} (day)	GEE
1996	−158 (−16, + 3)	441	605	−1203
1997	−153 (−32, + 22)	471	635	−1259
1998	−131 (−23, + 5)	541	709	−1381
1999	−178 (−16, + 4)	523	680	−1382
2000	−271 (−16, + 20)	503	676	−1449
2001	−175 (−25, + 23)	540	726	−1442
2002	−154 (−18, + 15)	481	647	−1282
Mean	−174	500	665	−1339
Standard deviation	46	38	42	94

All values in units of $g\,C\,m^{-2}\,yr^{-1}$. Nominal NEE values are calculated based on nocturnal data when $u_* > 0.25\,m\,s^{-1}$, with bracketed values indicating the NEE range calculated with $u_* > 0.20$ and $u_* > 0.30\,m\,s^{-1}$. Other parameters are calculated based on $u_* > 0.25\,m\,s^{-1}$.
NEE, net ecosystem C exchange.

Statistical analysis of variability in NEE

Statistical analysis of multiyear data sets provides another approach for understanding interannual variability in C exchange analysis. In this case, the goal may be to determine whether there are relationships between C exchange variables and readily available

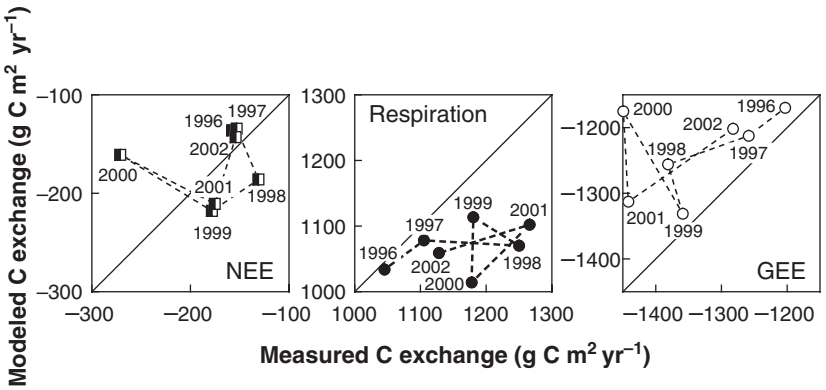

Fig. 8 Comparison of measured and modeled annual components of ecosystem C exchange. Modeled C exchange was not correlated with measured values.

meteorological data, or whether there are time dependencies in certain processes. As an example of the latter, Barford *et al*. (2001) carried out a lag-correlation analysis of monthly Harvard Forest data and found that anomalously high rates of summer C uptake were correlated with high respiration rates in the preceding January and February. We use the same general approach of relating monthly C exchange anomalies to monthly climate anomalies.

At the Howland forest, the relationship between monthly temperature anomalies and NEE anomalies changes through the year (Fig. 9a). In January and February, positive temperature anomalies are correlated with greater respiration (positive NEE anomaly, therefore correlation coefficients >0) but by the beginning of the growing season (March and April) anomalously high temperatures are strongly correlated with anomalously high C uptake (negative NEE anomaly, $r<0$). The relationship between anomalously high temperatures and greater C uptake is also seen at the end of the growing season (November and December for the evergreen Howland forest). During summer, however, anomalously high temperatures are related to lower rates of C uptake (positive NEE anomaly) and the correlation coefficients are greater than zero. For the months of April, August, and September, the individual correlation coefficients are significant at the 10% level, with $P<0.005$ for the collective probability that high temperatures are correlated with enhanced C uptake at the beginning and end of growing season. Over summer months, the collective probability of a correlation between anomalously high temperatures and reduced C uptake is also <0.005.

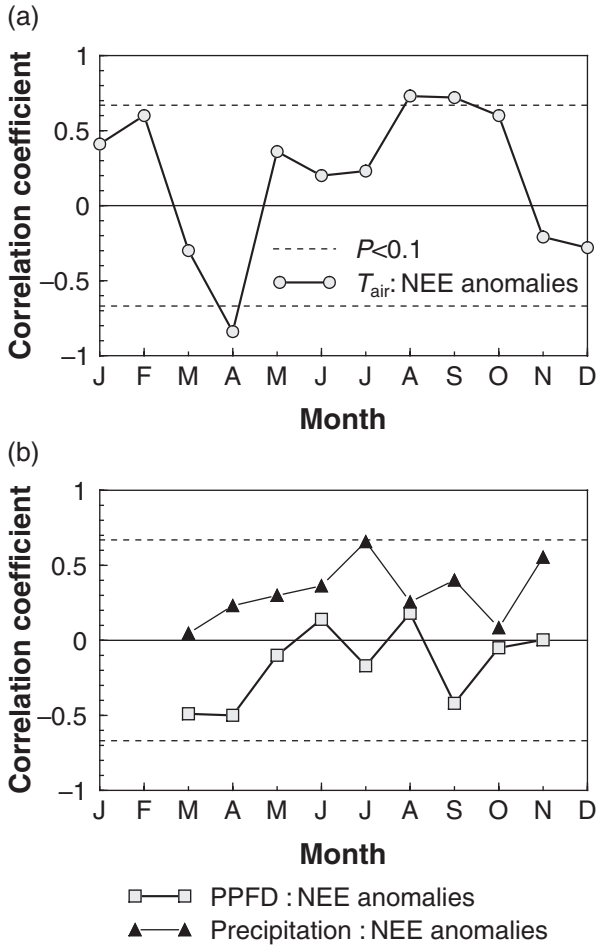

Fig. 9 (a) Correlation coefficients of air temperature and net ecosystem C exchange (NEE) flux anomalies by month. Anomalously large CO_2 uptake is seen for spring and late fall months that are warmer than normal. Reduced CO_2 uptake is seen in the late summer when temperatures are warmer than normal. The dashed line represents the threshold for correlation coefficients ($n=7$) that are significant at $P=0.10$. (b) Correlation coefficients of photosynthetically active photon flux density (PPFD) and NEE flux anomalies (squares) and precipitation and NEE flux anomalies (solid triangles) by month.

In contrast to the strong correlation of temperature and NEE anomalies, we observed no significant relationship between PPFD and NEE anomalies or between precipitation and NEE anomalies (Fig. 9b). This is somewhat curious given the strong half-hourly or daily relationship between PPFD and NEE. Similarly, Maine observed record-setting drought conditions in the summer of 2001, yet there is no relationship between summer precipitation anomalies and NEE. One possible explanation for the weak relationships between these variables and NEE is the correlated nature of the climate anomalies themselves (Fig. 10). In winter, clear sunny weather is associated with lower temperatures ($r<0$) while the opposite is true during the spring and summer. Not surprisingly, we observe an inverse correlation between PPFD and precipitation; anomalously wet months receive anomalously low levels of PPFD. In both cases, factors that by themselves have opposite effects on NEE (e.g. higher summer temperature and higher PPFD) are correlated, reducing the influence of the single variable.

Another reason for a lack of strong correlation between precipitation anomalies and NEE anomalies may be because in addition to the immediate impact of cloudiness, precipitation influences plant growth ultimately through soil moisture, which depends upon a variety of factors, including previous conditions. Using the soil water balance model BROOK90 (Federer *et al*., 2003), we found a significant, nonlinear relationship between soil moisture and summer NEE anomalies (Fig. 11). When soil moisture levels were too high or too low, net C uptake was less than at intermediate levels of soil moisture.

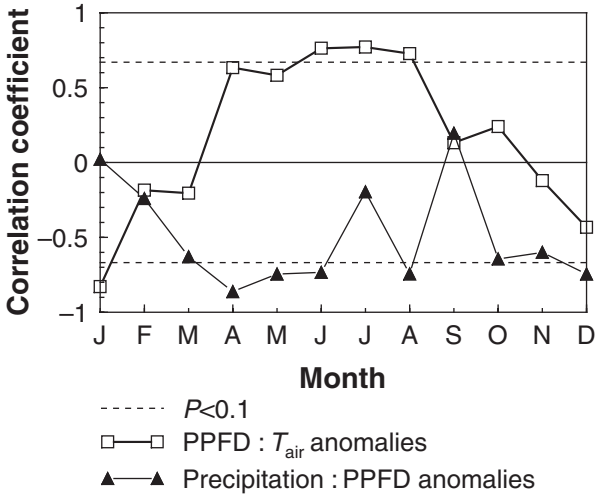

Fig. 10 Monthly photosynthetically active photon flux density (PPFD) and air temperature anomalies (open squares) and PPFD and precipitation anomalies (solid triangles) are significantly correlated. In winter, months that are brighter than the 7-year average are generally colder than normal (positive PPFD anomalies correlated with negative temperature anomalies) whereas in summer brighter than average months are usually warmer than normal (positive PPFD anomalies correlated with positive temperature anomalies). Months with above-average rainfall over the 7 years (positive precipitation anomaly) tend to be darker than average (negative PPFD anomaly).

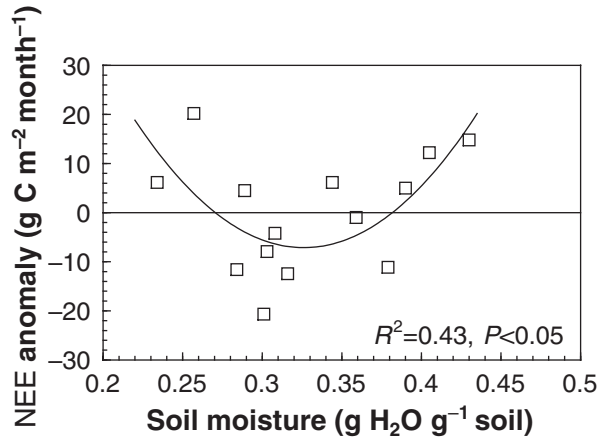

Fig. 11 July–August net ecosystem C exchange (NEE) anomalies are associated with soil moisture status. Reduced uptake is seen if soils are either too dry or too wet.

Discussion

Comparison with other sites

Howland forest's long-term average NEE of $\sim -174\,\mathrm{g\,C\,m^{-2}\,yr^{-1}}$ is somewhat lower than the average reported across the EUROFLUX sites of $-270\,\mathrm{g\,C\,m^{-2}\,yr^{-1}}$ (Janssens *et al.*, 2001) but in the range of values reported for other coniferous forest (see e.g. Carrara *et al.*, 2003). Mean Howland GEE and total ecosystem respiration at -1339 and $1165\,\mathrm{g\,C\,m^{-2}\,yr^{-1}}$, respectively, are close to the mean EUROFLUX values of -1380 and $1100\,\mathrm{g\,C\,m^{-2}\,yr^{-1}}$ (Table 2, Janssens *et al.*, 2001).

Annual net ecosystem exchange at the Howland forest varies by over 100%, ranging over the 1996–2002 period between -131 and $-271\,\mathrm{g\,C\,m^{-2}\,yr^{-1}}$ (Fig. 3, Table 3). This high level of interannual NEE variability appears to be common in other coniferous and deciduous forests (Goulden *et al.*, 1996a; 1998; Lindroth *et al.*, 1998; Lee *et al.*, 1999; Aubinet *et al.*, 2002; Carrara *et al.*, 2003) and should not be surprising given that it represents the difference between two much larger gross fluxes each controlled by somewhat different factors.

In previous work, observed interannual variability of forest C exchange has been related to springtime temperatures (Goulden *et al.*, 1996a; Black *et al.*, 2000), summer drought (Goulden *et al.*, 1996a), summer light levels (Goulden *et al.*, 1996a; Aubinet *et al.*, 2002), or length of growing season (Goulden *et al.*, 1996a; Carrara *et al.*, 2003). Only recently (Aubinet *et al.*, 2002; Carrara *et al.*, 2003) have climatic conditions been *statistically* related to variations in NEE. Here we have clearly demonstrated the relationship between anomalously warm spring months (and to a lesser extent anomalously warm autumn months) and enhanced C uptake. Summertime relations are more complicated and reflect the negative impact of high temperature and drought on NEE as well as the positive impact of PPFD.

An important result from analysis of the long-term record from the deciduous Harvard Forest (Barford *et al.*, 2001) is that anomalously high winter respiration rates were found to correlate with higher respiration rates the following summer. The authors hypothesized that winter snow cover significantly influenced rates of decomposition over many months. The authors also found that winter respiration anomalies were correlated with subsequent summer NEE uptake anomalies; higher rates of winter respiration were thus correlated with increased nocturnal respiration and daytime uptake. We performed a similar lag-correlation analysis of the Howland data (Fig. 12) but obtained different results. First, we did observe the strong serial autocorrelation between winter and early spring respiration (Fig. 12a) seen by Barford *et al.* (2001). However, summer month respiration rates were not correlated with previous winter respiration. Instead, autumn respiration rates at Howland tended to be inversely correlated with respiration rates from the previous winter. Litter input to the forest floor at Howland is

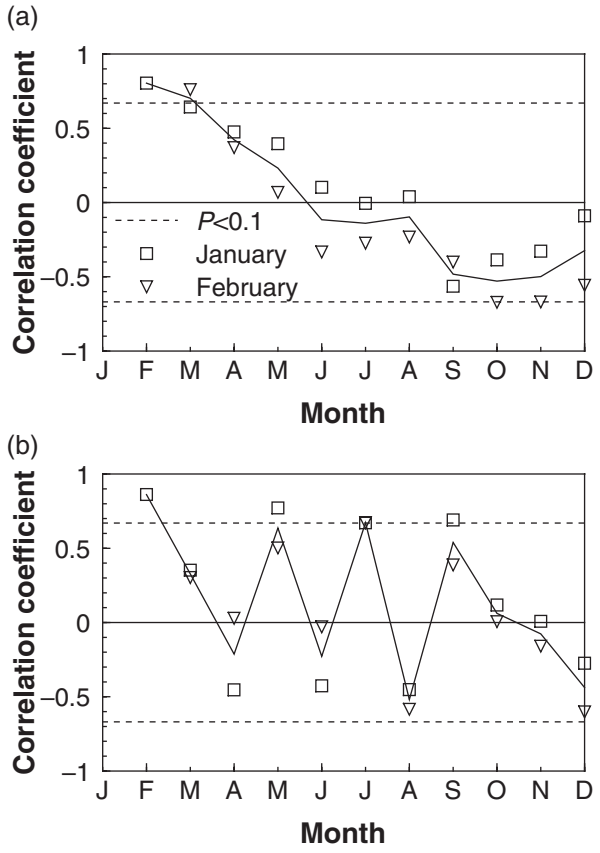

Fig. 12 Correlation analysis of January (square) or February (triangle) ecosystem respiration and subsequent month mean respiration (a) or net ecosystem C exchange (NEE) (b). Unlike Barford *et al*. (2001) we found no relationship between winter respiration and subsequent summer respiration or NEE.

more uniform than in a deciduous forest such as that investigated by the Harvard group. We speculate that at Howland and other coniferous forests, unusually high or low respiration rates early in the year will regulate the quantity of litter substrate leading to the opposite behavior later in the same year.

Also unlike Harvard forest, at Howland we found no relationship between winter respiration anomalies and subsequent summer NEE anomalies (Fig. 12b). To further explore the causes of NEE anomalies, we carried out additional lag-correlation analyses. We hypothesize that variability in ecological factors such as leaf area index or foliage nutrient status are likely to persist for several months and thus similarly influence NEE for several successive months; such variation in ecosystem state should be clearly visible in the lag-correlation structure. Results of these analyses are conflicting. There was no significant relationship between monthly respiration anomalies or NEE anomalies and NEE anomalies 1 month later over the whole data set (respiration : lagged NEE, $r = 0.11$, $P = 0.32$; NEE : lagged NEE, $r = -0.077$, $P = 0.49$). Examining the lag correlation by year, however, revealed that in both 1998 and 1999 monthly NEE anomalies were inversely ($r < 0$) correlated with those of the preceding month. Such an inverse behavior (also seen in Fig. 12b) is difficult to explain via ecological mechanisms. However, climatic fluctuations may show such patterns and we conclude that the absence of strong *positive* lag correlations in monthly NEE anomalies implies that these anomalies resulted more from climatic than ecological factors.

Our two-tower comparison found that fluxes measured from similar but distinct patches of forest were correlated at time scales ranging from hours to several years. Granier *et al*. (2002) compared fluxes from two European beech stands separated by ~ 900 km. Except for short-term differences (1–5 days) the temporal variation of NEE followed similar patterns at both beech sites. Differences in rainfall distribution within a year induced different degrees of water stress at both sites and accounted for some variation in annual NEE.

When we attempted to derive parameter values for simple physiological process models from half-hourly flux data, independent data from separate towers provided similar parameter estimates. This suggests that flux data can be used to parameterize simple (or not so simple) models of C exchange. However, parameter values for a simple model developed in the first year of measurement could not predict future variation of the large gross photosynthetic and respiratory fluxes with sufficient accuracy to make useful estimates of future NEE. It appears from these results (e.g. Fig. 8) that parameter values in this type of model may need to vary between years as well as during the growing season (Wang *et al*., 2003). Our earlier analysis of model parameters (Figs 4 and 6) shows just such variability. Why should model parameters change among or within years? The model evaluated here combines simple 'big-leaf' photosynthesis with total ecosystem respiration; key parameters are photosynthetic and respiratory capacities (P_{max} and A in Eqn (5)). Photosynthetic capacity is a combination of the amount of foliage, how it is displayed, and leaf biochemistry, while respiratory capacity represents a combination of auto- and heterotrophic pools. With such a simple structure, modest intra- or interannual variation in model parameters could result from a variety of physiological and ecological factors. Given the difficulty of predicting a small difference between the large photosynthetic and respiratory fluxes, such simple models appear to be of limited prognostic value and the challenge becomes one of determining what

drives seasonal and interannual variation in parameter values.

The model discussed here may also be deficient because it is missing some other factor(s) that, if included, would allow the other parameters to remain more nearly constant across years while simultaneously leading to more accurate model predictions. The analysis of monthly NEE anomalies suggests that summer drought may be one such factor worth investigating.

Conclusions

The strong correlation observed between the two towers at Howland leads us to conclude that the seasonal and interannual variations observed at flux sites are real manifestations of interactions between ecosystem processes and environmental drivers. Similarly, data from the two towers suggest that values of model parameters fit from flux data using least-squares techniques are robust and (relatively) precise. The two-tower system provides direct estimates of flux uncertainty that has been used to find model parameter values having the ML of fitting the observed data. Monte Carlo techniques produced additional likely parameter sets of simple models of photosynthesis and respiration, and analysis indicates that certain parameters are highly correlated. Use of flux data and the ML approach to extract information on the physiological processes of photosynthesis and respiration will doubtless prove valuable in future ecosystem carbon cycle studies.

An important result emerging from our two-tower comparison is that since climatic conditions are generally coherent across some hundreds of kilometers, regional C exchange, at least within a vegetation type, is also probably strongly coherent. This provides support to the idea that climatic influences on vegetation can result in regional-scale signals of surface–atmosphere CO_2 exchange (Goulden *et al*., 1996a; Granier *et al*., 2002).

Our analysis of interannual variability indicates what several of these regional-scale signals might be. Warmer spring temperatures, identified as a potential source of NEE variability in a boreal deciduous forest (Black *et al*., 2000), are significantly correlated with enhanced CO_2 uptake at this subboreal coniferous forest. A similar but weaker effect on NEE was seen for anomalously warm late autumn temperatures. By contrast, we found that anomalously warm months at the end of summer were significantly associated with anomalously low rates of C uptake. There was no significant relationship between light or precipitation anomalies and NEE anomalies. However, we did find that summer NEE anomalies were significantly related to soil moisture and that summer C uptake was reduced when soils were either too wet or too dry.

A simple, physiological model fit from flux data and driven by half-hourly values of light, air temperature, and soil temperature provided reasonable estimates of respiration, photosynthesis, and NEE for the year in which it was parameterized. However, when driven by subsequent year environmental conditions, this model provided no utility for predicting variations in C exchange. To properly predict C exchange we suggest that somewhat more complicated models utilizing seasonal variations in photosynthetic capacity and perhaps various C pools will be necessary. This lack of utility applies mostly to predictions of NEE, and results from this quantity being the difference of two large gross fluxes that were modeled independently.

Acknowledgements

We thank the International Paper Company Ltd for providing access to the research site in Howland, Maine. The Howland flux research was supported by the USDA Forest Service Northern Global Change Program, the Office of Science (BER), US Department of Energy, through the Northeast Regional Center of the National Institute for Global Environmental Change under Cooperative Agreement no. DE-FC03-90ER61010, and by the Office of Science (BER), US Department of Energy, Interagency Agreement no. DE-AI02-00ER63028. The Howland Forest multiyear CO_2 flux and climate data set is available at http://public.ornl.gov/ameriflux/Data/index.cfm subject to AmeriFlux 'Fair-use' rules.

References

Aubinet M, Heinesch B, Longdoz B (2002) Estimation of the carbon sequestration by a heterogeneous forest: night flux corrections, heterogeneity of the site and inter-annual variability. *Global Change Biology*, **8**, 1053–1071.

Baldocchi DD (2003) Assessing the eddy covariance technique for evaluating carbon dioxide exchange rates of ecosystems: past, present and future. *Global Change Biology*, **9**, 479–492.

Barford CC, Wofsy SC, Goulden ML *et al*. (2001) Factors controlling long- and short-term sequestration of atmospheric CO_2 in a mid-latitude forest. *Science*, **294**, 1688–1691.

Barr AG, Griffis TJ, Black TA *et al*. (2002) Comparing the carbon budgets of boreal and temperate deciduous forest stands. *Canadian Journal of Forest Research*, **32**, 813–822.

Bevington PR (1969) *Data Reduction and Error Analysis for the Physical Sciences*. McGraw-Hill, New York.

Black TA, Chen WJ, Barr AG *et al*. (2000) Increased carbon sequestration by a boreal deciduous forest in years with a warm spring. *Geophysical Research Letters*, **27**, 1271–1274.

Black TA, den Hartog G, Neumann HH *et al*. (1996) Annual cycles of water vapour and carbon dioxide fluxes in and above a boreal aspen forest. *Global Change Biology*, **2**, 219–230.

Carrara A, Kowalski AS, Neirynck J *et al*. (2003) Net ecosystem CO_2 exchange of mixed forest in Belgium over 5 years. *Agricultural and Forest Meteorology*, **119**, 209–227.

Carter GC, Ferrie JF (1979) A coherence and cross-spectral estimation program. In: *Programs for Digital Signal Processing* (ed. The Digital Signal Processing Committee of the IEEE ASSP Society IEEE Press, New York.

CoHort Software (2002) *CoStat 6 (http://www.cohort.com)*. CoHort Software, Monterey, CA, USA.

Federer CA, Vörösmarty C, Fekete B (2003) Sensitivity of annual evaporation to soil and root properties in two models of contrasting complexity. *Journal of Hydrometeorology*, **4**, 1276–1290.

Fernandez IJ, Rustad LE, Lawrence GB (1993) Estimating total soil mass, nutrient content, and trace metals in soils under a low elevation spruce-fir forest. *Canadian Journal of Soil Science*, **73**, 317–328.

Finn D, Lamb B, Leclerc MY *et al*. (1996) Experimental evaluation of analytical and Lagrangian surface-layer flux footprint models. *Boundary-Layer Meteorology*, **80**, 283–308.

Goulden ML, Daube BC, Fan S-M *et al*. (1997) Physiological responses of black spruce forest to weather. *Journal of Geophysical Research*, **102**, 28987–28996.

Goulden ML, Munger JW, Fan S-M *et al*. (1996a) CO_2 exchange by a deciduous forest: response to interannual climate variability. *Science*, **271**, 1576–1578.

Goulden ML, Munger JW, Fan S-M *et al*. (1996b) Measurements of carbon sequestration by long-term eddy covariance: methods and a critical evaluation of accuracy. *Global Change Biology*, **2**, 169–182.

Goulden ML, Wofsy SC, Harden JW *et al*. (1998) Sensitivity of boreal forest carbon balance to soil thaw. *Science*, **279**, 214–217.

Granier A, Pilegaard K, Jensen NO (2002) Similar net ecosystem exchange of beech stands located in France and Denmark. *Agricultural and Forest Meteorology*, **114**, 75–82.

Hammer Ø, Harper DAT, Ryan PD (2001) PAST: paleontological statistics software package for education and data analysis. *Palaeontologia Electronica*, **4**, 9pp. http://palaeo-electronica.org/2001_1/past/issue1_01.htm.

Hollinger DY, Goltz SM, Davidson EA *et al*. (1999) Seasonal patterns and environmental control of carbon dioxide and water vapor exchange in an ecotonal boreal forest. *Global Change Biology*, **5**, 891–902.

Hollinger DY, Kelliher FM, Byers JN *et al*. (1994) Carbon dioxide exchange between an undisturbed old-growth temperate forest and the atmosphere. *Ecology*, **75**, 134–150.

Hollinger DY, Kelliher FM, Schulze E-D *et al*. (1995) Initial assessment of multi-scale measures of CO_2 and H_2O flux in the Siberian taiga. *Journal of Biogeography*, **22**, 425–431.

Hollinger DY, Kelliher FM, Schulze E-D *et al*. (1998) Forest–atmosphere carbon dioxide exchange in eastern Siberia. *Agricultural and Forest Meteorology*, **90**, 291–306.

Horst TW (1997) A simple formula for attenuation of eddy fluxes measured with first-order-response scalar sensors. *Boundary-Layer Meteorology*, **82**, 219–233.

Horst TW (2000) On frequency response corrections for eddy covariance flux measurements. *Boundary-Layer Meteorology*, **94**, 517–520.

Horst TW, Weil JC (1992) Footprint estimation for scalar flux measurements in the atmospheric surface layer. *Boundary-Layer Meteorology*, **59**, 279–296.

Horst TW, Weil JC (1994) How far is far enough?: the fetch requirements for micrometeorological measurements of surface fluxes. *Journal of Atmospheric and Ocean Technology*, **11**, 1018–1026.

Janssens IA, Lankreijer H, Matteucci G *et al*. (2001) Productivity overshadows temperature in determining soil and ecosystem across European forests. *Global Change Biology*, **7**, 269–278.

Leclerc MY, Karipot A, Prabha T *et al*. (2003a) Impact of non-local advection on flux footprints over a tall forest canopy: a tracer flux experiment. *Agricultural and Forest Meteorology*, **115**, 17–34.

Leclerc MY, Meskhidze N, Finn D (2003b) Comparison between measured tracer fluxes and footprint model predictions over a homogeneous canopy of intermediate roughness. *Agricultural and Forest Meteorology*, **117**, 145–158.

Lee X (1998) On micrometeorological observations of surface-air exchange over tall vegetation. *Agricultural and Forest Meteorology*, **91**, 39–49.

Lee X, Fuentes JD, Staebler RM *et al*. (1999) Long-term observations of the atmospheric exchange of CO_2 with a temperate deciduous forest in southern Ontario, Canada. *Journal of Geophysical Research*, **104**, 15975–15984.

Lindroth A, Grelle A, Morén A-S (1998) Long-term measurements of boreal forest carbon balance reveal large temperature sensitivity. *Global Change Biology*, **4**, 443–450.

Lloyd J, Taylor JA (1994) On the temperature dependence of soil respiration. *Functional Ecology*, **8**, 315–323.

Massman WJ (2000) A simple method for estimating frequency response corrections for eddy covariance systems. *Agricultural and Forest Meteorology*, **104**, 185–198.

Massman WJ (2001) Reply to comment by Rannik on 'A simple method for estimating frequency response corrections for eddy covariance systems'. *Agricultural and Forest Meteorology*, **107**, 247–251.

Metropolis N, Rosenbluth AW, Rosenbluth MN *et al*. (1953) Equation of state calculations by fast computing machines. *Journal of Chemical Physics*, **21**, 1087–1092.

Moore CJ (1986) Frequency response corrections for eddy correlation systems. *Boundary-Layer Meteorology*, **37**, 17–35.

O'Brien DM (1987) Problems in interpretation of power spectra of cloud fields. *Journal of Geophysical Research (D)*, **92**, 5522–5532.

Panofsky HA, Dutton JA (1984) *Atmospheric Turbulence*. John Wiley & Sons, New York.

Press WH, Teukolsky SA, Vetterling WT *et al*. (1993) *Numerical Recipes in Fortran 77: The Art of Scientific Computing*. Cambridge University Press, New York.

Running SW, Baldocchi DD, Turner D *et al*. (1999) A global terrestrial monitoring network, scaling tower fluxes with ecosystem modeling and EOS satellite data. *Remote Sensing of the Environment*, **70**, 108–127.

Sakai RK, Fitzjarrald DR, Moore KE (2001) Importance of low-frequency contributions to eddy fluxes observed over rough surfaces. *Journal of Applied Meteorology*, **40**, 2178–2192.

Schmid HP (1994) Source areas for scalars and scalar fluxes. *Boundary-Layer Meteorology*, **67**, 293–318.

US Department of Agriculture, Forest Service (2002) Forest inventory and analysis national core field guide, Vol. 1: field data collection procedures for phase 2 plots, Version 1.6. US Department of Agriculture, Forest Service, Washington Office. Internal report. On file with: US Department of Agriculture, Forest Service, Forest Inventory and Analysis, Washington, DC.

van Wijk MT, Bouten W (2002) Simulating daily and half-hourly fluxes of forest carbon dioxide and water vapor exchange with a simple model of light and water use. *Ecosystems*, **5**, 597–610.

von Storch H, Zwiers FW (1999) *Statistical Analysis in Climate Research*. Cambridge University Press, New York.

Wang Q, Tenhunen J, Falge E *et al*. (2003) Simulation and scaling of temporal variation in gross primary production for coniferous and deciduous temperate forests. *Global Change Biology*, **10**, 37–51.

Young H, Ribe J, Wainwright K (1980) *Weight tables for tree and shrub species in Maine*. University of Maine Agricultural and Experimental Station Miscellaneous Report, 230, University of Maine, Orono, ME.

Appendix: Analysis of u_* threshold and atmospheric stability on nocturnal respiration

The nocturnal (half-hour time periods when the sun is below the horizon and the PPFD $<5\,\mu mol\,m^{-2}\,s^{-1}$) atmosphere at Howland is generally stable. Because the degree of stability affects flux transport, we classified atmospheric stability based on the Monin–Obukhov length, L (m), calculated after Panofsky & Dutton (1984) using

$$L = \frac{-1u_*^3 \rho c_p T_{air}}{kgH\,(1 + (0.07/\beta))}, \qquad \text{(A1)}$$

where u_* is the friction velocity, ρ is the air density, c_p is the specific heat of air at constant pressure, T_{air} is air temperature (K), k is the von Karman constant (= 0.41), g is the acceleration because of gravity, H is the sensible heat, and β is the Bowen ratio. We used the following classifications; very unstable (class 1), $-40 < L < 0$, moderately unstable (class 2), $-200 < L < -40$, slightly unstable (class 3), $L < -200$, slightly stable (class 4), $L > 220$, moderately stable (class 5), $40 < L < 220$, and very stable (class 6), $0 < L < 40$. Over the 7 years of measurement, more than 90% of the nocturnal half-hour time periods were classified as 'stable' (class 4–6) whereas only 28% of daytime periods were classified 'stable' (Fig. 13a). For nocturnal conditions characterized by a narrow temperature range, the measured CO_2 flux varies significantly with stability class. For example, for summer nights when $15\,^{\circ}C < T_{air} < 18\,^{\circ}C$, ecosystem CO_2 efflux varies by stability class from -0.68 to $6.45\,\mu mol\,m^{-2}\,s^{-1}$ (Table 4 and Fig. 13c), a negative respiration here suggesting nocturnal CO_2 uptake. Stability and u_* are related via Eqn (A1) (see also Table 4), and researchers have typically used an empirically

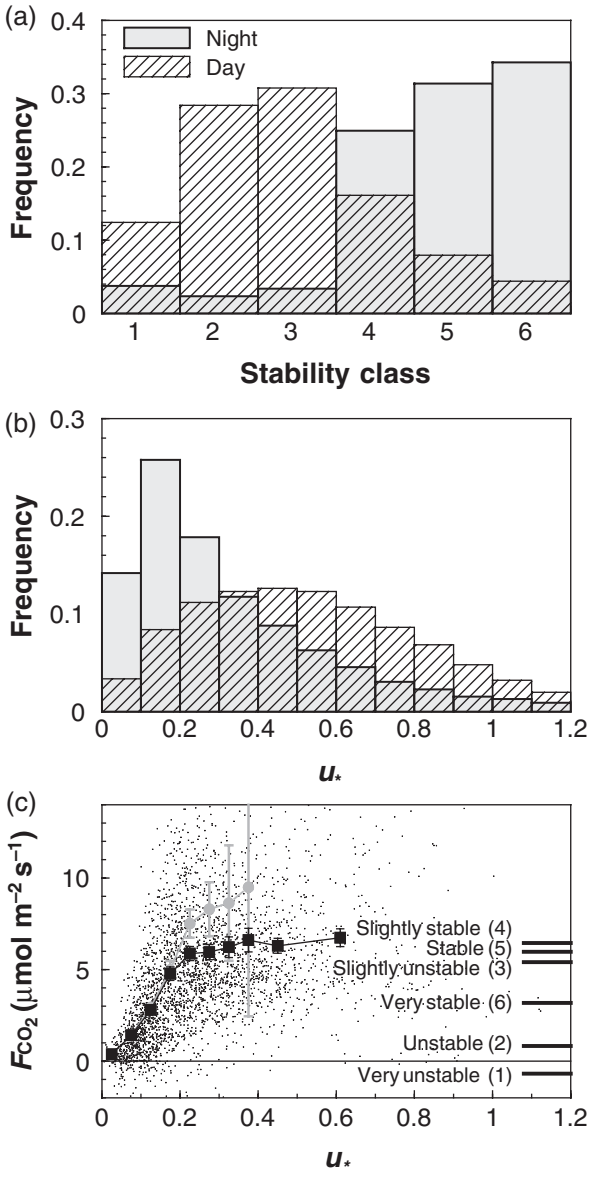

Fig. 13 (a) Frequency of occurrence of atmospheric stability classes, and (b) friction velocity (u_*) thresholds, by day and night at the Howland forest. The nocturnal atmosphere at Howland is characterized by stable conditions and low u_* values. (c) Nocturnal carbon dioxide (CO_2) flux for $15\,^{\circ}C < T_{air} < 18\,^{\circ}C$. The square symbols (± 95% confidence intervals) represent $0.05\,m\,s^{-1}$ u_* classes, and the lines on the right side of the figure are the means of the six stability classes. The light gray circles (± 95% confidence intervals) indicate mean flux values if the u_* during the preceding half-hour was $<0.2\,m\,s^{-1}$. Flux values are relatively constant with $u_* > 0.25$ and similar to values obtained for slightly or moderately stable conditions.

determined minimum u_* value to exclude conditions with poor transport. The daytime and night-time frequency distributions of u_* at Howland (Fig. 13b) are significantly different (χ^2 test, $P << 0.01$) with low

Table 4 Relationship between nocturnal stability class, u_*, and ecosystem respiration

Stability class	Respiration (σ)	u_* (σ)	n	Frequency
(1) Very unstable	−0.68 (6.09)	0.091 (0.069)	57	0.018
(2) Unstable	0.83 (7.16)	0.176 (0.082)	50	0.016
(3) Slightly unstable	5.41 (4.23)	0.348 (0.152)	136	0.044
(4) Slightly stable	6.45 (4.02)	0.481 (0.219)	621	0.199
(5) Stable	5.97 (4.13)	0.283 (0.105)	1066	0.341
(6) Very stable	3.18 (2.63)	0.135 (0.059)	1192	0.381
All data	4.77 (4.09)	0.263 (0.180)	3122	1

Data are restricted to half-hour periods when $15\,^{\circ}C < T_{air} < 18\,^{\circ}C$.

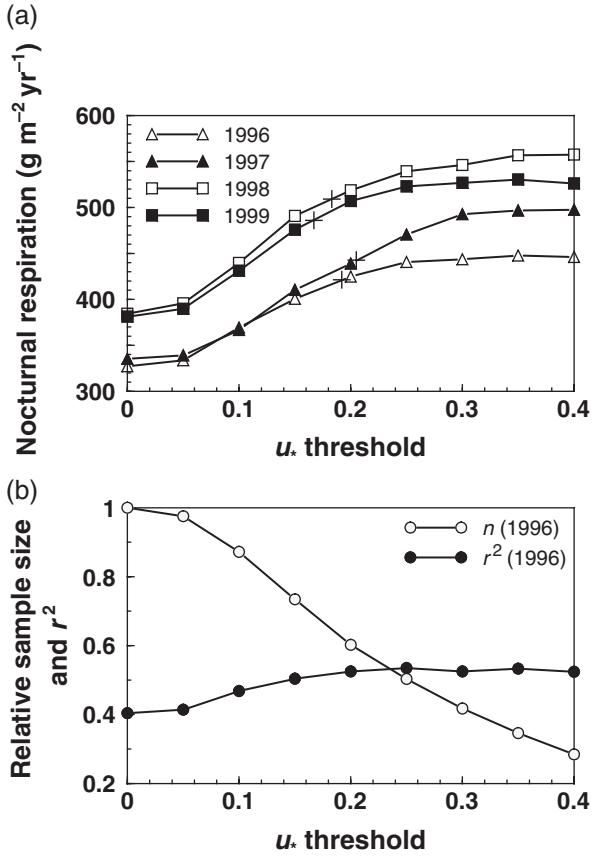

Fig. 14 (a) Annual estimates of nocturnal respiration as a function of u_* threshold for accepting data (only first 4 years shown for clarity). Estimates are relatively constant for $u_* > 0.25$. The crosses indicate annual nocturnal respiration estimate using an alternative acceptance criteria of stability classe 4 or 5. (b) Relative sample size (open circles) and squared correlation coefficient of respiration model fit to nocturnal data (closed circles) as a function of u_* threshold.

u_* conditions much more common in the night than day. Fully half of all nocturnal time periods are characterized by a $u_* < 0.25\,m\,s^{-1}$ while the daytime median u_* is $0.52\,m\,s^{-1}$.

Examining nocturnal respiration (the sum of eddy flux and storage flux) as a function of u_* at night over a narrow temperature range ($15\,^{\circ}C < T_{air} < 18\,^{\circ}C$), there appears to be a threshold value of about $0.25\,m\,s^{-1}$, above which mean nocturnal respiration is relatively constant (Fig. 13c). A stability class criteria (accepting data when stability is class 4 or 5) at Howland yields a nocturnal respiration value that is similar to that obtained with a u_* threshold of $0.25\,m\,s^{-1}$ (Fig. 13c; 6.13 ± 0.19 vs. $6.23 \pm 0.19\,\mu mol\,m^{-2}\,s^{-1}$, mean and 95% confidence intervals). One caution with using u_* thresholds is the risk of setting a threshold too high. At Howland, we found that there can be transient storage of CO_2 in the canopy airspace not tracked by the conventionally measured storage flux (= integral of half-hourly CO_2 change in the air column below the instrumentation) and that anomalously high nocturnal efflux can occur when time periods with abundant turbulence ($u_* > 0.25\,m\,s^{-1}$) followed more quiescent periods (Fig. 13c). The specific criteria or threshold used for accepting or rejecting data during nocturnal periods has an effect on the annual estimate of respiration (Fig. 14) and thus NEE. We find that on an annual basis, a criteria of stability class 4 or 5 provides an estimate of nocturnal respiration similar to that obtained with a $u_* > 0.2\,m\,s^{-1}$. Based on these and the preceding results, we use nocturnal data from half-hour time periods when u_* exceeds $0.25\,m\,s^{-1}$ for our nominal estimates of NEE, but because the exact threshold is vague, we bracket our estimates of NEE with similar calculations using u_* thresholds of 0.20 and $0.30\,m\,s^{-1}$.